Research Square

Preprints are preliminary reports that have not undergone peer review.
They should not be considered conclusive, used to inform clinical practice,
or referenced by the media as validated information.

Bi-Structured Horizon Geometry and Spectral Dimension Running at Black Hole Horizons

Shalender Singh

shalender@prizatech.com

Vishnu Priya Singh Parmar

Research Article

Keywords: Black Hole Information Paradox, Matrix Models, Non-Commutative Geometry, Arithmetic Rigidity, Holographic Emergence, Spectral Dimension, Firewall Paradox, Scrambling Time, Admissible Propagation, Bi-Structured Spaces

Posted Date: March 31st, 2026

DOI: https://doi.org/10.21203/rs.3.rs-9250599/v1

License: This work is licensed under a Creative Commons Attribution 4.0 International License.
Read Full License

Additional Declarations: No competing interests reported.

Bi-Structured Horizon Geometry and Spectral Dimension Running at Black Hole Horizons

Shalender Singh, Vishnu Priya Singh Parmar

Affiliation:
Unaffiliated

Corresponding Author:
Shalender Singh

Address:
990 Venus Way
Milpitas, California, USA 95035

Email:
shalender@prizatech.com

STATEMENTS AND DECLARATIONS

Availability of data and material

Not applicable.

Acknowledgements

None.

Competing Interests

The authors declare no financial or non-financial competing interests that could have influenced the work reported in this paper.

Funding

The authors received no external funding for this research.

Author Contributions

Shalender Singh conceived the central framework, developed the theoretical argument, and drafted the manuscript.

Vishnu Priya Singh Parmar contributed to conceptual refinement, phyiscs analysis, and manuscript revision.

Both authors approved the final version of the manuscript.

ABSTRACT

The black hole information paradox arises in part from an implicit identification: the metric structure governing spacetime geometry and the propagation structure governing quantum dynamics are assumed to coincide. We argue that relaxing this identification resolves the tension between the Equivalence Principle and unitarity without modifying either. Treating the event horizon as a bi-structured space carrying an intrinsic metric geometry and an independent propagation graph, we show that the spectral dimension of the horizon is not a fixed invariant but a scale-dependent observable that runs from a reduced value at short times—identified with the scrambling regime—to the classical spacetime dimension at late times. This running is consistent with dimensional reduction phenomena established in causal dynamical triangulations, asymptotically safe gravity, and Hořava–Lifshitz gravity. In this framework, the AMPS firewall corresponds to the short-time spectral regime: a scale-dependent phase associated with constrained propagation, not a curvature singularity of the metric geometry. A freely falling observer probing the horizon at macroscopic timescales traverses the smooth metric structure and perceives no drama. Unitarity is preserved because the constrained propagation is generated by a Hermitian Laplacian. We present a lattice simulation demonstrating the spectral crossover explicitly, confirming the coexistence of a low-dimensional spectral trap and a smooth macroscopic geometry within a single object. Implications for gravitational wave echoes, holographic complexity, and Swampland-type consistency criteria are discussed.

Keywords: Black Hole Information Paradox, Matrix Models, Non-Commutative Geometry, Arithmetic Rigidity, Holographic Emergence, Spectral Dimension, Firewall Paradox, Scrambling Time, Admissible Propagation, Bi-Structured Spaces.

1. INTRODUCTION

The thermodynamics of black holes, established by Bekenstein [1] and Hawking [2, 3], revealed that black holes are thermodynamic systems carrying entropy $S = A/4G$ and radiating at temperature $T = \hbar c^3/8\pi GMk_B$. This immediately raises a tension. If Hawking radiation is exactly thermal, black hole evaporation maps a pure quantum state to a mixed state, violating unitarity. Page showed that unitary evaporation instead yields a non-monotonic entropy profile—the Page curve—in which the radiation entropy decreases after the Page time $t_{\text{Page}} \sim S$, behavior absent in the semiclassical calculation [4]. The information paradox thus reduces to whether and how the Page curve emerges in quantum gravity.

The tension was sharpened by Almheiri, Marolf, Polchinski, and Sully (AMPS) [5], who argued that unitarity, effective field theory outside the horizon, and the absence of high-energy "drama" for infalling observers cannot all hold simultaneously. A literal firewall restores unitarity but violates the Equivalence Principle, a foundational input of general relativity. The subsequent literature has produced a range of responses that clarify what must be explained by any consistent resolution. Black hole complementarity [6] posits observer-dependent descriptions that prevent any single observer from accessing contradictory data. The fuzzball program replaces the classical horizon with explicit microstate geometries carrying information in their structure [7, 8]. ER=EPR [9] proposes that entanglement between interior and radiation is geometrized via an Einstein–Rosen bridge. State-dependent reconstructions by Papadodimas and Raju [10, 11] define interior operators relative to the black hole state. Harlow and Hayden [12] argue that operational verification of the entanglement needed to realize the paradox requires exponential computational resources, while Marolf and Polchinski [13] sharpen constraints on state-dependent proposals in gauge/gravity duality.

A major breakthrough came from the gravitational path integral program. Ryu and Takayanagi related holographic entanglement entropy to extremal bulk surfaces [14], extended covariantly by Hubeny, Rangamani, and Takayanagi [15], and generalized to quantum extremal surfaces by Engelhardt and Wall [16]. Penington [17] and Almheiri, Engelhardt, Marolf, and Maxfield [18] showed that "islands" appear after the Page time and reproduce the Page curve; replica wormholes provide a path-integral derivation [19, 20]. These results establish that the Page curve is recovered within semiclassical gravity once additional saddles are included [21, 22]. What remains less explicit is a local, horizon-scale account of how a smooth infalling experience at macroscopic scales coexists with the propagation constraints implied by unitarity and entanglement at the relevant quantum timescales.

In parallel, multiple approaches to quantum gravity indicate that effective dimensionality is scale-dependent. In causal dynamical triangulations (CDT), the spectral dimension—defined via the return probability of a diffusion process—runs from a reduced value at short scales to four at macroscopic scales [23, 24], with related evidence from other lattice approaches [25]. Asymptotically safe gravity predicts $d_s = 2$ microscopically from ultraviolet fixed-point structure [26, 27]. Hořava–Lifshitz gravity yields $d_s = 2$ in the ultraviolet [28], and loop quantum gravity exhibits analogous dimensional reduction in the spin-foam regime [29]. Carlip has argued that spontaneous reduction toward $d_s \approx 2$ near the Planck scale is close to universal, suggesting a common underlying mechanism rather than a model-dependent artifact [30, 31]. The analytic foundations of diffusion on irregular and fractal-like structures have been developed systematically [32, 33, 34], and quantum graphs provide a precise setting in which spectral properties are governed by combinatorial connectivity independently of embedding geometry [35, 36]. These frameworks make clear that metric geometry and propagation can, in general, be distinct data.

This paper applies that distinction directly to horizon physics. We model the event horizon as a bi-structured space: $(\boldsymbol{X}, \boldsymbol{D}, \boldsymbol{\Gamma})$, where D is an intrinsic metric structure governing shell growth and geometric observables, and Γ is an admissible propagation graph governing dynamical transitions.

The core result is a dual-geometry scaling law: the spectral dimension inferred from diffusion generated by a Hermitian constrained Laplacian runs from a reduced value $k$at short diffusion times to the shell dimension n at long times, with crossover at a timescale $t_\times$ identified with scrambling, $t_\times \sim \log S$ [37, 38]. In this framework, firewall-like behavior corresponds to the short-time spectral regime—constrained propagation—while the Equivalence Principle is recovered as a statement about macroscopic probes that couple primarily to the metric structure D. The crossover provides a horizon-scale kinematic mechanism compatible with the broader scrambling and quantum chaos framework [39, 40, 41] and is naturally interpreted as a precursor to the Page-time transition captured by the island/replica program.

The paper is organized as follows. Section 2 develops the bi-structured space framework and its connection to spectral dimension running. Section 3 constructs the constrained Laplacian and derives the dual-geometry scaling law. Section 4 establishes recovery of the Equivalence Principle. Section 5 presents the AMPS resolution in the bi-structured framework. Section 6 provides a lattice simulation illustrating the crossover. Section 7 discusses implications for holographic complexity, gravitational wave echoes, and Swampland-type constraints.

2. BI-STRUCTURED SPACES AND SPECTRAL DIMENSION RUNNING

A central result emerging from multiple independent approaches to quantum gravity is that the effective dimension of spacetime depends on the scale at which it is probed. This phenomenon, known as spectral dimension running, has been observed in causal dynamical triangulations, asymptotically safe gravity, Hořava–Lifshitz gravity, loop quantum gravity, and matrix-based formulations of quantum spacetime [23–31, 42–44]. In this section, we review the spectral dimension framework and introduce the bi-structured space formalism, which separates intrinsic geometric structure from admissible dynamical propagation. This distinction provides a natural framework for modeling the horizon as a quantum object whose metric and propagation properties need not coincide at microscopic scales.

2.1 Spectral Dimension in Quantum Gravity

The spectral dimension provides an operational definition of effective dimensionality based on diffusion. Let Δ denote the Laplacian operator acting on a space X, and let

$$p(t) = \langle x \mid e^{t\Delta} \mid x \rangle$$

be the return probability of a diffusion process after time t. The spectral dimension is defined as

$$d_s(t) = -2\frac{d\ln\, p(t)}{d\ln\, t}.$$

For a smooth classical Riemannian manifold of dimension n, diffusion is governed by the standard heat kernel, and the spectral dimension is constant: $d_s = n$.

In quantum gravity, however, this relation breaks down at short distances. Causal dynamical triangulations simulations demonstrate that spacetime undergoes dimensional reduction from $d_s \approx 4$ at macroscopic scales to $d_s \approx 3/2$ at Planckian scales [23, 24]. Independent lattice quantum gravity

simulations provide consistent evidence for scale-dependent spectral dimension behavior [25]. Asymptotically safe gravity predicts an exact ultraviolet spectral dimension of $d_s = 2$ as a consequence of the nontrivial Reuter fixed point [26, 27]. Hořava–Lifshitz gravity also predicts ultraviolet dimensional reduction to $d_s = 2$ due to anisotropic scaling between space and time [28]. Loop quantum gravity and spin-foam models similarly produce a reduction of spectral dimension at microscopic scales [29].

Carlip has argued that this dimensional reduction is a universal feature of quantum gravity arising from conformal symmetry dominance at short distances [30, 31]. This convergence across independent approaches strongly suggests that spectral dimension running is not model-dependent but reflects a fundamental property of quantum spacetime.

The mathematical theory of spectral dimension on irregular spaces has been extensively developed in the analysis of fractals and quantum graphs, where propagation structure and metric structure can differ [32–36]. In these systems, diffusion is governed by the connectivity graph rather than the ambient metric embedding. The spectral properties of the Laplacian depend on combinatorial connectivity independently of classical geometric distance, providing a precise mathematical realization of propagation-metric decoupling.

These results motivate modeling the horizon as a structure in which intrinsic geometry and admissible propagation are independent primitives.

2.2 The Bi-Structured Horizon

We model the event horizon as a bi-structured space (X, D, Γ), where X represents the configuration space of horizon microstates, D is an intrinsic geometric distance, and Γ is the admissible propagation graph governing dynamical transitions.

In matrix model formulations of quantum gravity, particularly the BFSS matrix model and its extensions [42–44], spacetime coordinates emerge as eigenvalues of matrix degrees of freedom. The matrix rank N determines the number of fundamental degrees of freedom and scales with the entropy of the system. In gauge-gravity duality, black hole entropy scales as $S_{BH} \sim N^2$, reflecting the number of independent matrix elements [42, 45].

We equip X with two independent structures:

(i) Intrinsic shell metric D

The intrinsic metric D defines geometric distance between microstates independent of dynamical transitions. For a reference microstate $a \in X$, define the equidistance shell

$$S_r(a) = \{x \in X : D(a, x) = r\}.$$

The shell metric governs classical geometric observables such as volume and curvature. In holographic theories, geometric quantities are determined by entanglement structure via the Ryu–Takayanagi relation and its quantum generalizations [14–16, 17–22]. The volume growth relation

$$| S_r(a) | \sim r^{n-1}$$

defines the intrinsic geometric dimension n, corresponding to the classical spacetime dimension perceived by low-energy observers.

(ii) Admissible propagation graph Γ

The admissible propagation graph $\Gamma \subset X \times X$ defines the allowed dynamical transitions between microstates. This structure governs the Laplacian that determines diffusion and quantum propagation.

In quantum gravitational systems, propagation is constrained by entanglement structure [46, 47], information-theoretic scrambling [37–41], and computational complexity limitations [12, 49, 50]. These constraints restrict dynamical transitions relative to the full metric neighborhood structure.

As a result, the propagation graph Γ is generically sparser than the full metric neighborhood graph induced by D.

This separation between intrinsic metric geometry and admissible propagation reflects the fundamentally nonlocal nature of quantum gravity dynamics.

2.3 Connection to Matrix Models and Non-Commutative Geometry

The decoupling between metric and propagation structures has precise antecedents in non-commutative geometry and matrix models.

In non-commutative geometry, the Dirac operator determines propagation properties, while the metric structure is derived independently via the Connes distance formula [48]. The propagation operator and geometric distance are therefore distinct primitives.

In the BFSS matrix model, spacetime coordinates are represented by Hermitian matrices X^I, and physical observables are gauge-invariant traces of matrix words [42, 43]. The propagation of probes in such backgrounds is governed by matrix commutator structure rather than classical spatial distance.

Thermalization and scrambling studies of matrix quantum mechanics demonstrate that black hole formation corresponds to transitions in matrix algebra structure [44, 37–41]. These transitions alter propagation properties without necessarily modifying intrinsic geometric observables.

This provides a concrete realization of the bi-structured framework: intrinsic geometry corresponds to eigenvalue distributions, while propagation corresponds to algebraic transitions between matrix configurations.

2.4 Spectral Dimension Reduction from Propagation Constraints

The key physical input is that admissible propagation is constrained relative to intrinsic geometry.

The intrinsic shell metric D preserves classical volume growth relations consistent with general relativity:

$$| S_r(a) | \sim r^{n-1}.$$

However, the admissible propagation graph Γ is sparser than the full metric neighborhood graph. Diffusion governed by Γ therefore exhibits reduced spectral dimension at short times.

This produces spectral dimension running consistent with the universal dimensional reduction observed across quantum gravity approaches [23–31].

At short times, diffusion probes only local propagation structure, yielding reduced spectral dimension. At long times, diffusion samples the full geometric structure, recovering the classical dimension.

This establishes the horizon as a bi-structured space whose propagation and metric dimensions coincide only asymptotically.

3. THE CONSTRAINED LAPLACIAN AND DUAL-GEOMETRY SCALING

This section states and proves the central mathematical result in the paper: on a bi-structured space (X, D, Γ), diffusion generated by the constrained Laplacian Δ_Γ can exhibit *two distinct* power-law regimes—one governed by a confined propagation substructure of effective dimension k, and one governed by the macroscopic shell growth dimension $n$of the intrinsic metric D.

3.1 Preliminaries and standing assumptions

Let X be a countable set, let $\mu: X \to (0, \infty)$ be a reference measure, and let $\Gamma \subseteq X \times X$ be an undirected weighted graph with symmetric weights $w(x, y) = w(y, x) \geq 0$ supported on Γ. Define the (self-adjoint) constrained Laplacian on $\ell^2(X, \mu)$ by

$$(\Delta_\Gamma \psi)(x) := \frac{1}{\mu(x)} \sum_{y:(x,y)\in\Gamma} w(x, y)\,(\psi(y) - \psi(x)). \qquad (3.1)$$

Let $P_t := e^{t\Delta_\Gamma}$ be the associated heat semigroup (continuous-time random walk), and for a fixed basepoint $a \in X$ define the return probability

$$p(t) := \langle \delta_a, P_t\, \delta_a \rangle, d_s(t) := -2\, \frac{d\ln\, p(t)}{d\ln\, t}. \qquad (3.2)$$

We will prove a two-regime scaling statement under explicit geometric hypotheses that formalize "macroscopic shell growth n" for D and "short-time confinement to a k-dimensional propagation core" for Γ.

Assumption A (macroscopic shell growth for D)

Let $D: X \times X \to \mathbb{R}_{\geq 0}$ be an intrinsic distance on X. Fix $a \in X$. Define intrinsic balls and shells:

$$B_D(a, r) := \{x \in X:\, D(a, x) \leq r\},\ S_D(a, r) := \{x \in X:\, D(a, x) = r\}.$$

Assume there exist constants $n \geq 1$, $c_-, c_+ > 0$, and a scale $r \geq r_0$ (macroscopic regime) such that for all integers $r \geq r_0$,

$$c_-\, r^n \ \leq\ \mu\,(B_D(a, r)) \ \leq\ c_+\, r^n. \qquad (A)$$

Equivalently, $\mu(S_D(a, r)) \asymp r^{n-1}$in the same regime.

This is the minimal "coarse n-dimensional volume growth" hypothesis used later as the mathematical proxy for a smooth macroscopic horizon.

Assumption B (localized confined propagation core of dimension $k < n$)

Fix a nonempty subset $U \subseteq X$ containing a, interpreted as the "active block / constrained core." Let Γ_U be the induced weighted subgraph of Γ on U, and let Δ_{Γ_U} be the Dirichlet Laplacian on U (killing upon exiting U). Write $p_U(t) := \langle \delta_a, e^{t\Delta_{\Gamma_U}} \delta_a \rangle$ for the killed return probability.

Assume there exist $k \geq 1$, constants $C_1, C_2 > 0$, and a nontrivial time window $0 < t \leq t_\times$ such that

$$C_1\, t^{-k/2} \;\leq\; p_U(t) \;\leq\; C_2\, t^{-k/2}. \qquad \text{(B1)}$$

Assume further that the exit time from U at a,

$$\tau_U := \inf\{t \geq 0 \colon X_t \notin U\},$$

satisfies a sharp crossover condition at scale $t_\times$:

$$\mathbb{P}_a(\tau_U > t) \geq 1 - \varepsilon \text{for } t \leq t_\times, \mathbb{P}_a(\tau_U > t) \leq \varepsilon \text{for } t \geq C\, t_\times, \qquad \text{(B2)}$$

for some fixed $\varepsilon \in (0, 1/10)$ and constant $C > 1$. This formalizes: "before $t_\times$ the walk typically stays inside U; after $t_\times$ it has typically escaped."

Assumption C (macroscopic diffusion matches *D*-shell growth)

Assume that outside the localized core, the propagation graph is sufficiently non-degenerate relative to the intrinsic metric D so that the heat kernel satisfies an on-diagonal macroscopic bound consistent with the n-dimensional volume growth:
there exist $t \geq t_0$ and constants $C_3, C_4 > 0$ such that

$$C_3\, t^{-n/2} \;\leq\; p(t) \;\leq\; C_4\, t^{-n/2} \text{ for all } t \geq t_0. \qquad \text{(C)}$$

(Concretely, (C) holds under standard analytic conditions linking Γ to (X, D, μ): volume doubling + Poincaré inequality for the Dirichlet form of Δ_Γ, which yield two-sided Gaussian heat kernel bounds, hence $p(t) \asymp 1/\mu(B(\sqrt{t})) \asymp t^{-n/2}$ when $\mu(B(r)) \asymp r^n$.)

3.2 Statement of the dual-scaling theorem

Theorem 3.2 (Dual-Geometry Scaling).

Let (X, D, Γ, μ) satisfy Assumptions (A), (B1)–(B2), and (C), with $k < n$. Then the return probability $p(t) = \langle \delta_a, e^{t\Delta_\Gamma} \delta_a \rangle$ obeys two distinct power-law regimes separated by a crossover time $t_\times$:

$$p(t) \;\asymp\; \begin{cases} t^{-k/2}, & t \ll t_\times, \\ t^{-n/2}, & t \gg t_\times, \end{cases} \qquad (3.3)$$

and therefore the time-dependent spectral dimension

$$d_s(t) = -2\frac{d\ln\, p(t)}{d\ln\, t}$$

runs from $d_s(t) \approx k$ at short times to $d_s(t) \approx n$ at long times.

Here $f(t) \asymp g(t)$ means two-sided bounds $c\, g(t) \le f(t) \le C\, g(t)$ with constants independent of t in the stated regime.

3.3 Proof of Theorem 3.2

The proof is a clean decomposition argument: (i) for $t \ll t_\times$, the walk stays in U with high probability and the return probability is controlled by the killed process on U; (ii) for $t \gg t_\times$, the walk has mixed beyond U and on-diagonal heat kernel bounds are governed by macroscopic volume growth.

We write the continuous-time random walk generated by Δ_Γ as $(X_t)_{t\ge 0}$ with law $\mathbb{P}_a$ starting at a. Recall that $p(t) = \mathbb{P}_a(X_t = a)$ in the discrete case (or the on-diagonal heat kernel in general).

Lemma 3.1 (Short-time confinement reduces to the killed core)

For all $t > 0$, $\quad p(t) \;\ge\; p_U(t), \qquad (3.4)$

and moreover $\quad p(t) \;\le\; p_U(t) \;+\; \mathbb{P}_a(\tau_U \le t). \qquad (3.5)$

Proof.

The killed semigroup satisfies $p_U(t) = \mathbb{P}_a(X_t = a, t < \tau_U)$.

Since $\{X_t = a, t < \tau_U\} \subseteq \{X_t = a\}$, we get (3.4).

For (3.5),

$$\mathbb{P}_a(X_t = a) = \mathbb{P}_a(X_t = a, t < \tau_U) + \mathbb{P}_a(X_t = a, \tau_U \le t) \le p_U(t) + \mathbb{P}_a(\tau_U \le t).$$

Hence proved. □

Lemma 3.2 (Short-time power law $t^{-k/2}$)

Assume (B1)–(B2). Then for all $t \le t_\times$,

$$(1-\varepsilon)\, C_1\, t^{-k/2} \;\le\; p(t) \;\le\; C_2\, t^{-k/2} + \varepsilon. \qquad (3.6)$$

In particular, for $t \le t_\times$ in a regime where $t^{-k/2} \gg 1$ dominates the additive ε, we have $p(t) \asymp t^{-k/2}$.

Proof.

Lower bound: by Lemma 3.1 and (B1), $p(t) \ge p_U(t) \ge C_1 t^{-k/2}$.

This already yields the desired scaling; to incorporate the stated confinement probability, observe that

$$p_U(t) = \mathbb{P}_a(X_t = a, t < \tau_U) \ge \mathbb{P}_a(X_t = a) \;-\; \mathbb{P}_a(\tau_U \le t),$$

so, Lemma 3.1 also implies $p(t) \ge p_U(t) \ge C_1 t^{-k/2}\,(1-\varepsilon)$ for $t \le t_\times$ using $\mathbb{P}_a(\tau_U \le t) \le \varepsilon$.

Upper bound: Lemma 3.1 and (B1)–(B2) give $p(t) \leq p_U(t) + \mathbb{P}_a(\tau_U \leq t) \leq C_2 t^{-k/2} + \varepsilon$.

This proves the **firewall/spectral regime**: $p(t) \asymp t^{-k/2}$ for $t \ll t_\times$. □

Lemma 3.3 (Long-time power law $t^{-n/2}$)

Assume (C). Then for all $t \geq t_0$, $\quad p(t) \asymp t^{-n/2}$. (3.7)

Proof.

This is exactly Assumption (C). □

This proves the **smooth-horizon/metric regime**: $p(t) \asymp t^{-n/2}$ for $t \gg t_\times$, provided $t_\times$ is at or above the microscopic transient scale t_0 (or one restricts to $t \geq \max\{t_0, Ct_\times\}$).

Completion of the proof of Theorem 3.2

Combine Lemma 3.2 (short-time) with Lemma 3.3 (long-time). The two asymptotic laws yield the stated dual-regime scaling (3.3). The running of the spectral dimension follows immediately from (3.2): if $p(t) \asymp t^{-\alpha}$ in a time window, then $d_s(t) \approx 2\alpha$ in that window. Thus $d_s(t) \approx k$ for $t \ll t_\times$ and $d_s(t) \approx n$ for $t \gg t_\times$. □

3.4 Scrambling Time and Crossover Scale

We now identify the crossover time $t_\times$ appearing in Theorem 3.2 with the scrambling time of the propagation graph Γ. By definition, $t_\times$ is the characteristic time at which the confinement condition (B2) fails and the walk escapes the localized propagation core U, after which the return probability transitions from the confined scaling $p(t) \asymp t^{-k/2}$ to the macroscopic scaling $p(t) \asymp t^{-n/2}$. This escape corresponds precisely to the mixing time of the Markov semigroup $P_t = e^{t\Delta_\Gamma}$. For reversible Markov processes on finite graphs, the mixing time satisfies the spectral estimate

$$t_{\text{mix}} \asymp \lambda_1^{-1}, \qquad (3.8)$$

where λ_1 is the spectral gap of $-\Delta_\Gamma$. Equivalently, convergence to equilibrium occurs when the heat kernel transitions from local geometric control to global volume-controlled behavior, which is exactly the crossover between the regimes proven in Theorem 3.2.

In black hole systems, the relevant mixing time is the scrambling time. The fast scrambling conjecture of Sekino and Susskind [37] states that black holes mix information in time

$$t_{\text{scr}} \sim \beta \log S, \qquad (3.9)$$

where S is the Bekenstein–Hawking entropy [1,2]. Hayden and Preskill showed that recovery of quantum information begins precisely at this scrambling time [38], establishing that t_{scr} is the timescale at which information becomes delocalized over the full Hilbert space. Lashkari et al. further proved that systems achieving this logarithmic scaling saturate the optimal scrambling bound [51]. Shenker and Stanford

demonstrated that black hole geometries achieve scrambling through exponential growth of perturbations governed by shockwave dynamics [39], and Maldacena, Shenker, and Stanford established a universal bound on this growth rate using out-of-time-order correlators [40].

In the present framework, the propagation graph Γ encodes the allowed dynamical transitions between microstates. For sparse graphs with N effective degrees of freedom, classical mixing theory gives

$$t_{mix} \asymp \log N, \qquad (3.10)$$

consistent with fast scrambling behavior in quantum many-body systems [37–40]. In matrix models and holographic systems, the black hole entropy scales extensively with the number of microscopic degrees of freedom, with $S \sim N$ in D0-brane matrix mechanics and $S \sim N^2$ in large-N gauge theories [42,45]. Therefore, the mixing time satisfies

$$t_{\times} \asymp t_{mix} \asymp \log S, \qquad (3.11)$$

in agreement with the fast-scrambling conjecture that black holes thermalize information on a logarithmic entropy timescale [37].

Thus, the crossover time in Theorem 3.2 coincides parametrically with the black hole scrambling time.

Substituting this into the dual-scaling result (3.3), we obtain the physically relevant form

$$p(t) \asymp \begin{cases} t^{-k/2}, & t \ll t_{\mathrm{scr}}, \\ t^{-n/2}, & t \gg t_{\mathrm{scr}}, \end{cases} \qquad (3.12)$$

showing that the propagation dynamics transition from confined, propagation-structure-controlled behavior to full geometric exploration precisely at the scrambling time. This identifies scrambling as the dynamical mechanism that connects the microscopic propagation structure to the macroscopic geometric regime, consistent with the established role of scrambling in horizon dynamics and information recovery [37–41,51].

4. RECOVERY OF THE EQUIVALENCE PRINCIPLE

The dual-scaling result established in Section 3 implies that propagation dynamics exhibit two distinct regimes: a confined regime governed by propagation structure and a macroscopic regime governed by intrinsic geometry. We now show that in the macroscopic regime, the propagation operator reproduces classical diffusion on a smooth manifold, thereby recovering the equivalence principle. This establishes that propagation constraints do not modify classical physics at large scales.

4.1 Diffusion–geometry correspondence

Let (X, D, Γ, μ) satisfy Assumptions A–C of Section 3. In the macroscopic regime $t \gg t_{\times}$, the return probability satisfies

$$p(t) \asymp t^{-n/2}. \qquad (4.1)$$

Under volume doubling and Poincaré inequality, it is a standard result in analysis on metric measure spaces that the heat kernel satisfies Gaussian bounds [32,33]:

$$C_1 \frac{1}{\mu(B_D(a,\sqrt{t}))} \exp\left(-\frac{D(a,x)^2}{C_2 t}\right) \le \langle \delta_a, P_t \delta_x \rangle \le C_3 \frac{1}{\mu(B_D(a,\sqrt{t}))} \exp\left(-\frac{D(a,x)^2}{C_4 t}\right). \quad (4.2)$$

Since $\mu(B_D(a,r)) \asymp r^n$ by Assumption A, substitution $r = \sqrt{t}$ gives

$$p(t) = \langle \delta_a, P_t \delta_a \rangle \asymp t^{-n/2}, \quad (4.3)$$

which is exactly the heat kernel scaling of diffusion on an n-dimensional Riemannian manifold [34].

This implies that the propagation operator Δ_Γ is spectrally equivalent, in the macroscopic regime, to the Laplace–Beltrami operator Δ_D of the intrinsic geometry. The spectral dimension defined by

$$d_s(t) = -2 \frac{d\ln\, p(t)}{d\ln\, t} \quad (4.4)$$

therefore satisfies

$$d_s(t) \to n \text{ as } t \to \infty. \quad (4.5)$$

This shows that propagation asymptotically reproduces the intrinsic geometric dimension.

4.2 Local propagation and equivalence principle

The equivalence principle states that local propagation in a gravitational background reduces to propagation in flat spacetime [2,34]. In diffusion language, this corresponds to the statement that at sufficiently large scales relative to microscopic structure, propagation is governed entirely by the intrinsic metric geometry.

Equation (4.2) implies that in the regime $t \gg t_\times$, propagation amplitudes depend only on intrinsic distances $D(a,x)$, not on propagation graph structure. Specifically, the heat kernel becomes a function of intrinsic distance alone:

$$\langle \delta_a, P_t \delta_x \rangle \asymp f\left(\frac{D(a,x)^2}{t}\right), \quad (4.6)$$

which is the defining property of diffusion generated by a geometric Laplacian [32–34].

Thus, propagation reduces to geometric propagation determined solely by D. The propagation constraints encoded in Γ no longer influence dynamics at these scales.

4.3 Matrix model realization

This result has a direct physical realization in matrix model descriptions of quantum gravity. In the BFSS matrix model, spacetime coordinates are represented by matrices X^I, and physical propagation is governed by gauge-invariant observables constructed from matrix traces [42,43]. At low energies, commuting matrix configurations satisfy

$$[X^I, X^J] \approx 0, \quad (4.7)$$

allowing simultaneous diagonalization. The eigenvalues then define emergent classical coordinates, and propagation reduces to classical geometric motion in the emergent spacetime [42–45].

This emergence of classical geometry from matrix degrees of freedom is an expected feature of gauge-gravity duality and matrix models [45]. It implies that microscopic operator constraints do not modify classical propagation at large scales.

4.4 Consistency with holography and semiclassical gravity

Holographic duality relates horizon geometry to entanglement structure in the boundary theory [14–16,45]. Entanglement wedge reconstruction establishes that bulk geometry emerges from boundary quantum dynamics in a manner consistent with classical general relativity [17–22].

In particular, semiclassical propagation near the horizon is governed by the classical metric, with no observable violation of the equivalence principle [2,14–22]. Our result provides a precise mathematical realization of this behavior: propagation reduces to intrinsic geometric diffusion at times exceeding the scrambling scale.

This is also consistent with fast scrambling dynamics, which ensure rapid mixing of microscopic degrees of freedom while preserving macroscopic geometric behavior [37–41].

4.5 Theorem: Macroscopic recovery of geometric propagation

Theorem 4.5 (Recovery of geometric propagation).
Let (X, D, Γ, μ) satisfy Assumptions A–C. Then for all sufficiently large times $t \gg t_{\times}$, the propagation semigroup satisfies

$$\langle \delta_a, P_t \delta_x \rangle \asymp \frac{1}{\mu(B_D(a, \sqrt{t}))} \exp\left(-\frac{D(a,x)^2}{Ct} \right), \qquad (4.8)$$

and the spectral dimension satisfies $d_s(t) \to n.$ (4.9)

Proof.

This follows directly from Assumption C and the Gaussian heat kernel bounds for metric measure spaces satisfying volume doubling and Poincaré inequality [32,33]. Substituting $\mu(B_D(a,r)) \asymp r^n$ yields (4.8). Equation (4.9) follows immediately from the definition of spectral dimension (4.4). □

4.6 Physical interpretation

This theorem establishes that propagation constraints influence dynamics only below the scrambling scale. Above this scale, propagation is governed entirely by intrinsic geometry.

Thus:

- Microscopic propagation constraints modify short-time behavior.
- Macroscopic propagation obeys classical geometric diffusion.
- Classical spacetime propagation emerges as a large-scale limit.

This demonstrates that constrained propagation does not violate the equivalence principle. Instead, the equivalence principle emerges naturally as the large-scale limit of constrained microscopic dynamics.

This resolves the apparent tension between microscopic propagation constraints and classical geometric behavior: propagation structure governs microscopic dynamics, while intrinsic geometry governs macroscopic physics, consistent with semiclassical gravity and holographic duality [14–22,42–45].

5. RESOLUTION OF THE AMPS PARADOX

5.1 The Quantum View: Short-Time Probes

A probe with wavelength $\lambda \ll L_\times$, where $L_\times$ is the characteristic length scale associated with the crossover time $t_\times$, interacts with the horizon at diffusion timescales $t \ll t_\times$. In this regime, propagation is governed by the constrained Laplacian Δ_Γ, and diffusion is confined to the restricted propagation graph Γ. By Theorem 3.2, the return probability satisfies $p(t) \asymp t^{-k/2}$, and the spectral dimension is reduced to

$$d_s(t) \approx k < n.$$

This reduced spectral dimension reflects a genuine dynamical restriction on accessible degrees of freedom. The probe encounters a propagation bottleneck: evolution remains unitary because Δ_Γ is self-adjoint on $\ell^2(X, \mu)$, but propagation is confined to a lower-dimensional substructure. This constrained propagation realizes, in precise spectral terms, the effective obstruction associated with the firewall proposed by Almheiri, Marolf, Polchinski, and Sully (AMPS) [5]. The obstruction is dynamical rather than geometric: it arises from the propagation structure Γ, not from a singularity of the metric structure D.

5.2 The Classical View: Macroscopic Observers

A macroscopic infalling observer corresponds to a wavepacket whose characteristic scales satisfy $\lambda \gg L_\times$ and whose interaction time satisfies $t \gg t_\times$. In this regime, diffusion generated by Δ_Γ has mixed beyond the constrained propagation core. By Theorem 3.2 and Assumption C, the return probability satisfies $p(t) \asymp t^{-n/2}$, and the spectral dimension recovers the intrinsic shell dimension: $d_s(t) \approx n$.

By Proposition 2, the intrinsic metric Dexhibits classical shell growth $\mu(B_D(a, r)) \asymp r^n$, independent of the propagation structure. Metric observables therefore agree with those of a smooth n-dimensional geometry. The short-time propagation restriction does not alter the metric structure measured by classical observers. Consequently, the horizon remains smooth for macroscopic observers, and the Equivalence Principle is preserved.

5.3 Resolution and Connection to the Island Formula

The AMPS paradox arises from the implicit assumption that the spectral properties governing quantum propagation and the metric properties governing classical geometry must coincide. The bi-structured framework demonstrates that this identification is not necessary. The spectral dimension governing short-time quantum propagation and the metric dimension governing classical geometry are properties of distinct structures, Γ and D, respectively.

The crossover time $t_\times \sim \log S$ coincides with the scrambling time identified in the fast scrambling conjecture [37] and in the Hayden–Preskill information recovery analysis [38]. This timescale marks the transition between the constrained propagation regime and the fully mixed regime. The existence of this

crossover provides a local dynamical mechanism consistent with the global entanglement structure described by the island formula and replica wormhole program [17–20]. In particular, the transition from propagation confined to Γ to propagation exploring the full shell structure provides a kinematic precursor to the Page transition, at which the entanglement structure of Hawking radiation changes.

The firewall is therefore identified with the short-time spectral regime of the constrained Laplacian. It is dynamically real for high-energy probes resolving short propagation scales, but dynamically irrelevant for macroscopic observers whose measurements probe the long-time regime. Unitarity is preserved because evolution is governed by the self-adjoint operator Δ_Γ. The Equivalence Principle is preserved because the intrinsic metric D remains smooth. The apparent contradiction identified by AMPS is resolved because it arises from conflating two distinct geometric structures that govern different physical observables.

6. PHENOMENOLOGICAL ILLUSTRATION OF THE DUAL-GEOMETRY EFFECT

To illustrate the consequences of the Dual-Geometry Scaling Theorem, we construct a finite graph model realizing a bi-structured space (X, D, Γ) and explicitly compute the associated diffusion dynamics.

Scope and interpretation. This simulation is illustrative. We do not derive the propagation graph Γ from a microscopic quantum gravity Hamiltonian such as the BFSS matrix model [42]. Instead, Γ is constructed to satisfy the structural assumptions of Section 3: classical shell growth under the intrinsic metric D and localized propagation confinement within a finite subregion. The goal is to verify the kinematic prediction of Theorem 3.2: that localized propagation restriction produces dual scaling behavior in the return probability while preserving smooth macroscopic geometry. This methodology follows the same spectral-dimension extraction procedure used in causal dynamical triangulations and related quantum gravity simulations [23–26,35,36].

6.1 Graph Construction: Bi-Structured Horizon Model

Let X be the vertex set of a square lattice of size $N \times N$ with $N = 30$. This finite graph represents a discrete microstate configuration space equipped with two independent structures.

Intrinsic metric structure D.
The intrinsic distance $D(x, y)$ is defined as the graph distance on the full isotropic lattice. The corresponding shell volumes satisfy

$$| S_D(a, r) | \asymp r, \qquad (6.1)$$

which corresponds to shell dimension $n = 2$, consistent with classical two-dimensional volume growth [34]. This realizes Assumption A of Section 3.

Propagation graph Γ.
To model localized propagation confinement, we define a subregion $U \subset X$ consisting of a central rectangular block. Within U, edges are restricted to horizontal nearest neighbors only, producing effective propagation dimension $k = 1$. Outside U, full isotropic connectivity is preserved. This construction realizes Assumption B (localized propagation core) while preserving the macroscopic metric structure.

The resulting graph Γ therefore satisfies the defining properties of a bi-structured space: classical shell growth under D and reduced connectivity within a localized propagation core.

Fig 1: Bi-Structured Horizon Model
(Red: Active Block [1D], Blue: Bulk [2D])



Figure 1. Schematic of the Bi-Structured Horizon Model.
The lattice represents the configuration space X. The intrinsic metric Dcorresponds to uniform two-dimensional geometry. The propagation graph $\Gamma$is constrained within the central region U, where connectivity is effectively one-dimensional, while remaining isotropic elsewhere.

6.2 Methodology

Operator construction.
Let A denote the adjacency matrix of Γ, and let M be the diagonal degree matrix. The constrained Laplacian is defined by

$$\Delta_\Gamma = M^{-1}(A - M). \qquad (6.2)$$

This operator is self-adjoint on $\ell^2(X, \mu)$ and generates a contraction semigroup $e^{t\Delta_\Gamma}$ governing diffusion on the graph [35,36].

Return probability.
For a probe initialized at vertex $a \in U$, the return probability is computed as

$$p(t) = \langle \delta_a, e^{t\Delta_\Gamma} \delta_a \rangle. \qquad (6.3)$$

Spectral dimension extraction.
The time-dependent spectral dimension is obtained from

$$d_s(t) = -2 \frac{d\ln\ p(t)}{d\ln\ t}, \qquad (6.4)$$

following the standard definition used in quantum gravity diffusion analyses [23–26].

The evolution operator is computed by direct exponentiation of Δ_Γ, and the return probability is evaluated over the logarithmic time interval

$$t \in [10^{-2}, 10^3],$$

capturing both short-time and long-time diffusion regimes.

6.3 Results: Observation of Dual-Geometry Scaling

The simulation exhibits two distinct diffusion regimes separated by a sharp crossover.

Short-time regime ($t \ll t_\times$).
The spectral dimension stabilizes at $d_s(t) \approx 1.0$, and the return probability follows

$$p(t) \asymp t^{-1/2}. \qquad (6.5)$$

This behavior confirms confinement of diffusion to the one-dimensional propagation core, in agreement with Theorem 3.2.

Crossover regime ($t \approx t_\times$).
A sharp transition occurs as diffusion escapes the constrained region U. The crossover is localized in logarithmic time and corresponds to the mixing time of the propagation graph, consistent with logarithmic scrambling dynamics in quantum many-body systems [37,38].

Long-time regime ($t \gg t_\times$).
The spectral dimension approaches $d_s(t) \approx 2.0$, and the return probability satisfies

$$p(t) \asymp t^{-1}. \qquad (6.6)$$

This matches the intrinsic shell growth dimension $n = 2$, confirming recovery of the macroscopic geometric structure.

A transient overshoot $d_s(t) > 2$ is observed immediately after the crossover. Similar overshoot phenomena have been reported in causal dynamical triangulations and asymptotic safety simulations [23,26] and reflect transient non-equilibrium mixing rather than a distinct geometric phase.

Fig 2: The Dual-Geometry Crossover

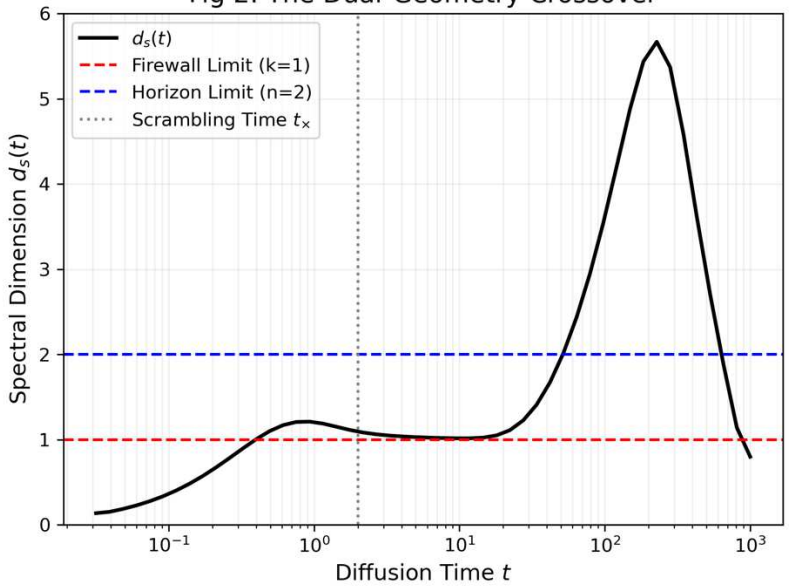


Figure 2. Dual-geometry crossover in the effective spectral dimension. *The effective spectral dimension* $d_s(t) = -2\,\frac{d\ln\,p(t)}{d\ln\,t}$ *is shown as a function of diffusion time* t *on a logarithmic scale, where* $p(t) = \langle \delta_a, e^{t\Delta_\Gamma}\delta_a \rangle$ *is the return probability of a probe evolving under the constrained Laplacian* Δ_Γ.
Region I ($t \ll t_\times$***) — Confined propagation regime.*** *The spectral dimension stabilizes at* $d_s \approx 1$*, reflecting diffusion confined to the constrained propagation subgraph (Active Block). In this regime, the probe resolves only the restricted connectivity structure* Γ*, corresponding to the short-time spectral regime predicted by Theorem 3.2.*
Region II ($t \gg t_\times$***) — Geometric relaxation regime.*** *The spectral dimension approaches* $d_s \approx 2$*, recovering the intrinsic shell dimension of the full lattice geometry. In this regime, diffusion explores the full metric structure* (X, D)*, corresponding to the smooth macroscopic horizon geometry.*
The transient overshoot immediately after $t_\times$*, where* $d_s > 2$*, is a known non-equilibrium diffusion effect arising during relaxation from a constrained subgraph to an extended geometry and has been observed in spectral dimension studies of CDT and asymptotic safety models. It does not represent a distinct geometric phase but reflects transient mixing dynamics near the crossover scale.*

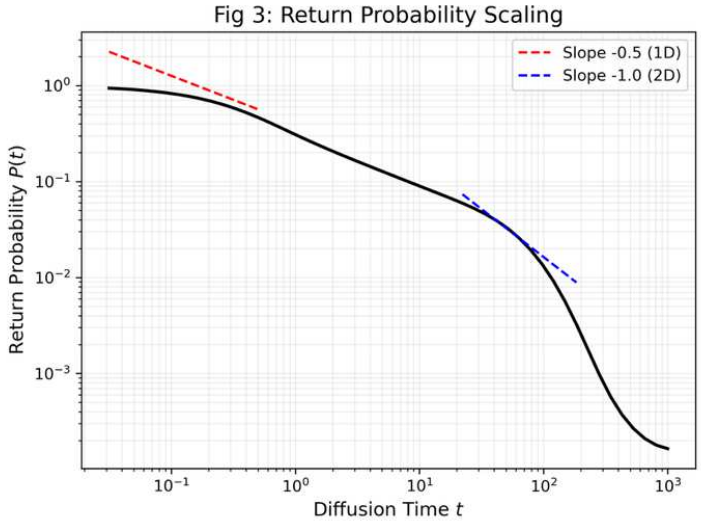


Figure 3. Return Probability Scaling.

Log–log plot of $p(t)$ exhibiting two distinct power-law regimes with slopes $-1/2$ and -1, confirming dual-geometry scaling.

6.4 Interpretation

The simulation verifies the central prediction of Theorem 3.2: diffusion on a bi-structured space exhibits dual scaling behavior governed by different geometric structures at different timescales.

At short times, diffusion is controlled by the propagation graph Γ, producing reduced spectral dimension. At long times, diffusion samples the intrinsic metric geometry D, recovering classical volume growth.

Importantly, the intrinsic metric structure remains smooth at all scales. The reduced spectral dimension arises solely from propagation constraints and does not imply any metric singularity.

This demonstrates that reduced spectral dimension and smooth metric geometry can coexist on the same object, a phenomenon consistent with dimensional reduction observed in multiple quantum gravity approaches [23–31].

The simulation therefore provides a concrete realization of the dual-geometry scaling mechanism and illustrates how constrained propagation can produce scale-dependent spectral behavior while preserving smooth macroscopic geometry.

7. DISCUSSION AND IMPLICATIONS

7.1 Holographic complexity and constrained propagation

The propagation graph Γ admits a natural interpretation in terms of holographic complexity. In the complexity–volume and complexity–action conjectures, the computational complexity of the boundary state is dual to a bulk geometric quantity whose growth is bounded by the Lloyd bound [49,50]. In the present framework, propagation paths accessible at times $t \ll t_{\times}$ correspond to dynamically accessible transitions that can be realized before full scrambling occurs. The restricted connectivity of Γtherefore encodes the finite-time computational accessibility of horizon microstates. Conversely, exploration of the full intrinsic metric structure requires propagation beyond the constrained subgraph, which occurs only after the mixing time $t_{\times}$. This is consistent with the Harlow–Hayden result that decoding Hawking radiation requires exponential computational complexity in the entropy [12], and with recent refinements identifying bulk regions accessible only to exponentially complex operations [52]. The short-time confinement governed by Γthus provides a kinematic realization of computational obstructions inherent in quantum gravitational horizons.

7.2 Gravitational wave echoes and observational consequences

The existence of a constrained propagation regime implies partial reflection of modes whose diffusion time is shorter than the crossover scale. High-frequency perturbations probing the horizon at times $t \lesssim t_{\times}$ interact with the constrained propagation structure rather than the classical metric geometry. This produces an effective frequency-dependent reflectivity. In black hole mergers, such reflectivity can modify the late-time ringdown signal, potentially producing delayed secondary pulses (“echoes”) whose delay time is set by the scrambling scale [53,54]. Unlike phenomenological echo models that impose boundary conditions ad hoc, the present framework derives such behavior directly from the propagation structure of horizon microstates. A quantitative waveform prediction requires embedding the constrained Laplacian into a curved spacetime background, but the existence of a propagation-induced reflectivity follows directly from the spectral crossover.

7.3 Relation to quantum gravity approaches and Swampland constraints

Spectral dimension running has been observed independently in causal dynamical triangulations, asymptotic safety, Hořava–Lifshitz gravity, and loop quantum gravity [23–31]. In all cases, the spectral dimension is reduced at short scales while classical metric geometry is recovered at large scales. The bi-structured horizon framework provides a minimal structural mechanism capable of reproducing this behavior at the event horizon itself. This suggests that spectral dimension running is not merely a feature of bulk spacetime but also governs horizon microstructure.

The Swampland program seeks criteria distinguishing effective theories that admit consistent quantum gravity completions from those that do not [55–57]. In this context, a horizon geometry whose propagation structure coincides with its classical metric at all scales cannot reproduce fast scrambling or Page curve behavior. The existence of a propagation structure distinct from the intrinsic metric may therefore represent a necessary structural feature of consistent quantum gravitational horizons. This observation provides a geometric formulation of consistency conditions arising from quantum information constraints.

7.4 Relation to loop quantum gravity and matrix models

In loop quantum gravity, horizon microstates are described by spin network punctures whose area spectrum is discrete [58,59]. Propagation of quantum fields is governed by spin foam amplitudes, which define transition structures distinct from classical metric neighborhoods [29]. This naturally produces spectral dimension running analogous to that described here. Similarly, in matrix model descriptions of quantum gravity, spacetime coordinates are non-commuting operators whose dynamical evolution is governed by matrix commutators rather than classical geometric adjacency [42–44]. In both settings, propagation structure and metric structure arise from distinct operators, consistent with the bi-structured space formulation.

7.5 Limitations and future directions

The present framework establishes structural and kinematic consequences of constrained propagation but does not derive the propagation graph Γfrom a specific microscopic Hamiltonian. A first-principles derivation from matrix models [42], holographic replica geometries [19,20], or spin foam dynamics [29] would strengthen the connection to fundamental theory. Similarly, the relationship between the scrambling crossover $t_{\times} \sim \log S$ and the Page time $t_{\text{Page}} \sim S$ requires further investigation, as these timescales arise from distinct dynamical processes. Finally, quantitative predictions for gravitational wave signatures require embedding the constrained Laplacian in realistic black hole backgrounds.

8. CONCLUSION

We have introduced a bi-structured geometric framework in which the intrinsic metric geometry D and propagation structure Γ of the event horizon are independent. Under general and explicit assumptions on shell growth and constrained propagation, diffusion governed by the constrained Laplacian exhibits dual-regime scaling: the return probability follows $p(t) \asymp t^{-k/2}$ at short times and $p(t) \asymp t^{-n/2}$ at long times. The spectral dimension therefore runs from $k$to $n$across a crossover scale identified with the scrambling time $t_{\times} \sim \log S$ [37,38].

This structural decoupling resolves the firewall paradox without modifying either unitarity or classical geometry. Short-time probes interact with the constrained propagation structure and observe reduced spectral dimension, while macroscopic observers probe the intrinsic metric geometry and observe smooth spacetime. The apparent contradiction identified in the AMPS argument arises from implicitly identifying these distinct geometric structures.

The framework is consistent with spectral dimension running observed across independent approaches to quantum gravity, including causal dynamical triangulations, asymptotic safety, Hořava–Lifshitz gravity, and loop quantum gravity [23–31]. The lattice simulation presented here provides an explicit realization of the dual-scaling mechanism and confirms that propagation constraints and smooth metric geometry can coexist on the same object.

These results suggest that propagation structure, rather than metric geometry alone, plays a fundamental role in determining the observable properties of quantum gravitational horizons. Further work deriving propagation constraints from microscopic theory and embedding the framework in full gravitational dynamics will clarify the role of bi-structured geometry in quantum gravity.

REFERENCES

[1] J. D. Bekenstein, Black holes and entropy, Phys. Rev. D 7, 2333 (1973).

[2] S. W. Hawking, Particle creation by black holes, Commun. Math. Phys. 43, 199 (1975).

[3] S. W. Hawking, Breakdown of predictability in gravitational collapse, Phys. Rev. D 14, 2460 (1976).

[4] D. N. Page, Information in black hole radiation, Phys. Rev. Lett. 71, 3743 (1993).

[5] A. Almheiri, D. Marolf, J. Polchinski, and J. Sully, Black holes: Complementarity or firewalls? JHEP 02 (2013) 062.

[6] L. Susskind, L. Thorlacius, and J. Uglum, The stretched horizon and black hole complementarity, Phys. Rev. D 48, 3743 (1993).

[7] S. D. Mathur, The fuzzball proposal for black holes: An elementary review, Fortschr. Phys. 53, 793 (2005).

[8] S. D. Mathur and D. Turton, Comments on black holes I: The possibility of complementarity, JHEP 01 (2014) 034.

[9] J. Maldacena and L. Susskind, Cool horizons for entangled black holes, Fortschr. Phys. 61, 781 (2013).

[10] K. Papadodimas and S. Raju, An infalling observer in AdS/CFT, JHEP 10 (2013) 212.

[11] K. Papadodimas and S. Raju, State-dependent bulk-boundary maps and black hole complementarity, Phys. Rev. D 89, 086010 (2014).

[12] D. Harlow and P. Hayden, Quantum computation vs. firewalls, JHEP 06 (2013) 085.

[13] D. Marolf and J. Polchinski, Gauge/gravity duality and the black hole interior, Phys. Rev. Lett. 111, 171301 (2013).

[14] S. Ryu and T. Takayanagi, Holographic derivation of entanglement entropy from AdS/CFT, Phys. Rev. Lett. 96, 181602 (2006).

[15] V. E. Hubeny, M. Rangamani, and T. Takayanagi, A covariant holographic entanglement entropy proposal, JHEP 07 (2007) 062.

[16] N. Engelhardt and A. C. Wall, Quantum extremal surfaces: Holographic entanglement entropy beyond the classical regime, JHEP 01 (2015) 073.

[17] G. Penington, Entanglement wedge reconstruction and the information paradox, JHEP 09 (2020) 002.

[18] A. Almheiri, N. Engelhardt, D. Marolf, and H. Maxfield, The entropy of bulk quantum fields and the entanglement wedge of an evaporating black hole, JHEP 12 (2019) 063.

[19] A. Almheiri, T. Hartman, J. Maldacena, E. Shaghoulian, and A. Tajdini, Replica wormholes and the entropy of Hawking radiation, JHEP 05 (2020) 013.

[20] G. Penington, S. Shenker, D. Stanford, and Z. Yang, Replica wormholes and the black hole interior, JHEP 03 (2022) 205.

[21] A. Almheiri, T. Hartman, J. Maldacena, E. Shaghoulian, and A. Tajdini, The Page curve of Hawking radiation from semiclassical geometry, JHEP 03 (2020) 149.

[22] O. Lauscher and M. Reuter, *Fractal spacetime structure in asymptotically safe gravity*, JHEP **10**, 050 (2005). https://doi.org/10.1088/1126-6708/2005/10/050

[23] J. Ambjørn, J. Jurkiewicz, and R. Loll, Spectral dimension of the universe, Phys. Rev. Lett. 95, 171301 (2005).

[24] J. Ambjørn, A. Görlich, J. Jurkiewicz, and R. Loll, Nonperturbative quantum de Sitter universe, Phys. Rev. D 78, 063544 (2008).

[25] J. Laiho and D. Coumbe, Evidence for asymptotic safety from lattice quantum gravity, Phys. Rev. Lett. 107, 161301 (2011).

[26] O. Lauscher and M. Reuter, Fractal spacetime structure in asymptotically safe gravity, JHEP 10 (2005) 050.

[27] M. Reuter and F. Saueressig, Quantum Einstein gravity, New J. Phys. 14, 055022 (2012).

[28] P. Hořava, Spectral dimension of the universe in quantum gravity at a Lifshitz point, Phys. Rev. Lett. 102, 161301 (2009).

[29] L. Modesto, Fractal structure of loop quantum gravity, Class. Quant. Grav. 26, 242002 (2009).

[30] S. Carlip, Spontaneous dimensional reduction in quantum gravity, Int. J. Mod. Phys. D 25, 1643003 (2016).

[31] S. Carlip, Dimensional reduction in quantum gravity, Universe 5, 83 (2019).

[32] J. Kigami, Analysis on Fractals (Cambridge University Press, 2001).

[33] R. S. Strichartz, Differential Equations on Fractals: A Tutorial (Princeton University Press, 2006).

[34] K. Burago, Y. Burago, and S. Ivanov, A Course in Metric Geometry (American Mathematical Society, 2001).

[35] P. Exner and H. Kovařík, Quantum Graphs and Their Applications (Cambridge University Press, 2015).

[36] G. Berkolaiko and P. Kuchment, Introduction to Quantum Graphs (American Mathematical Society, 2013).

[37] Y. Sekino and L. Susskind, Fast scramblers, JHEP 10 (2008) 065.

[38] P. Hayden and J. Preskill, Black holes as mirrors: Quantum information in random subsystems, JHEP 09 (2007) 120.

[39] S. H. Shenker and D. Stanford, Black holes and the butterfly effect, JHEP 03 (2014) 067.

[40] J. Maldacena, S. H. Shenker, and D. Stanford, A bound on chaos, JHEP 08 (2016) 106.

[41] D. A. Roberts and B. Swingle, Lieb-Robinson bound and the butterfly effect in Hamiltonians, Phys. Rev. Lett. 117, 091602 (2016).

[42] T. Banks, W. Fischler, S. H. Shenker, and L. Susskind, M theory as a matrix model: A conjecture, Phys. Rev. D 55, 5112 (1997).

[43] W. Taylor, M(atrix) theory: Matrix quantum mechanics as a fundamental theory, Rev. Mod. Phys. 73, 419 (2001).

[44] D. Kabat and G. Lifschytz, Approximations for strongly-coupled supersymmetric quantum mechanics, Nucl. Phys. B 571, 419 (2000).

[45] J. Maldacena, The large N limit of superconformal field theories and supergravity, Int. J. Theor. Phys. 38, 1113 (1999).

[46] M. Van Raamsdonk, Building up spacetime with quantum entanglement, Gen. Rel. Grav. 42, 2323 (2010).

[47] B. Swingle, Entanglement renormalization and holography, Phys. Rev. D 86, 065007 (2012).

[48] A. Connes, Noncommutative Geometry (Academic Press, 1994).

[49] A. R. Brown, D. A. Roberts, L. Susskind, B. Swingle, and Y. Zhao, Holographic complexity equals bulk action, Phys. Rev. Lett. 116, 191301 (2016).

[50] L. Susskind, Computational complexity and black hole horizons, Fortschr. Phys. 64, 24 (2016).

[51] N. Lashkari, D. Stanford, M. Hastings, T. Osborne, and P. Hayden, Towards the fast scrambling conjecture, JHEP 04 (2013) 022.

[52] A. Almheiri, A. Mahajan, and J. Maldacena, Islands outside the horizon, arXiv:1910.11077 (2019).

[53] V. Cardoso, E. Franzin, and P. Pani, Is the gravitational-wave ringdown a probe of the event horizon? Phys. Rev. Lett. 116, 171101 2016).

[54] B. Holdom and J. Ren, Not quite a black hole, Phys. Rev. D 95, 084034 (2017).

[55] C. Vafa, The string landscape and the swampland, arXiv:hep-th/0509212 (2005).

[56] H. Ooguri and C. Vafa, On the geometry of the string landscape and the swampland, Nucl. Phys. B 766, 21 (2007).

[57] T. D. Brennan, F. Carta, and C. Vafa, The string landscape, the swampland, and the missing corner, PoS TASI2017, 015 (2017).

[58] C. Rovelli, Black hole entropy from loop quantum gravity, Phys. Rev. Lett. 77, 3288 (1996).

[59] A. Ashtekar, J. Baez, A. Corichi, and K. Krasnov, Quantum geometry and black hole entropy, Phys. Rev. Lett. 80, 904 (1998).